ChemComm

COMMUNICATION

View Article Online
View Journal | View Issue

Cite this: *Chem. Commun.*, 2021, **57**, 6094

Received 1st April 2021,
Accepted 14th May 2021

DOI: 10.1039/d1cc01747k

rsc.li/chemcomm

Immune evasion of SARS-CoV-2 variants of concern is driven by low affinity to neutralizing antibodies†

Matheus V. F. Ferraz, ‡[ab] Emerson G. Moreira, ‡[ab] Danilo F. Coêlho, ‡[ab] Gabriel L. Wallau ‡[a] and Roberto D. Lins ‡*[a]

SARS-CoV-2 VOC immune evasion is mainly due to lower cross-reactivity from previously elicited class I/II neutralizing antibodies, while increased affinity to hACE2 plays a minor role. The affinity between antibodies and VOCs is impacted by remodeling of the electrostatic surface potential of the Spike RBDs. The P.3 variant is a putative VOC.

The COVID-19 pandemic has dramatically impacted the world population since 2019 and currently accounts for more than 2 million deaths.[1] The genome evolution of its etiological agent, the severe acute respiratory syndrome coronavirus 2 (SARS-CoV-2), has been closely monitored since the rapid sharing of the first genomic sequences in December 2019.[2] SARS-CoV-2 shows a relatively low mutation rate compared to other RNA viruses, and hence few genomic sites accumulated mutations and were fixed until the second quarter of 2020. However, a substantially different scenario emerged between September–December 2020 with the detection of independent variants of concern (VOC) from different lineages, including B.1.1.7,[3] B.1.351,[4] and P.1,[5] bearing multiple amino acid replacements (K417T, E484K, and N501Y) and indels in the Spike protein,[4] which some researchers hypothesized to have occurred due to a "global shift in the SARS-CoV-2 selective landscape".[6] Although large-scale immunological studies are not available so far, the main hypothesis to explain such a global shift takes into account the rising population immunity, which would naturally select escape mutants with a higher fitness compared to previous circulating lineages. To support this hypothesis, some evidence could be mentioned, such as the increasing number of reinfection cases with VOCs and variants of interest (VOI) carrying some of the same amino acid mutation (E484K),[7] the continuous emergence of new VOIs carrying E484K and N501Y during the first months of 2021[8] and the recurrent emergence of some of those Spike amino acid changes in SARS-CoV-2 experimental evolution settings challenged with monoclonal and polyclonal antibodies.

To enter the host cell, SARS-CoV-2 makes use of the glycoprotein Spike (S). Protein S is a homotrimer and each monomer has two subunits, S1 and S2. The S1 subunit contains the receptor-binding domain (RBD), which binds to the human receptor angiotensin-converting enzyme 2 (hACE2), thus allowing the fusion of membranes and entry into the cell. Among the 29 SARS-CoV-2 encoded proteins, the S protein has been investigated more thoroughly due to its key role in hACE2 binding, and because the RBD region is one of the main targets of neutralizing antibodies (nAbs) produced from the human immunological response against SARS-CoV-2. By deep mutational scanning of the RBD region, it has been identified that most amino acid changes are deleterious for hACE2 binding, whereas a few marginally enhance the affinity to hACE2,[9] including some that have been detected in VOCs, such as N501Y in the more transmissible and mortal B.1.1.7 lineage. On the other hand, amino acid changes such as K417N, E484K, and N501Y found in VOCs P.1 and B.1.351[4] have been shown to increase viral fitness by lowering the effectiveness of neutralizing monoclonal and/or polyclonal antibodies.[8] Therefore, the emergence and spread of more fit VOC lineages may be driven by a mechanism other than the often-proposed affinity increase between hACE2 and SARS-CoV-2 Spike protein.

Despite the extensive description of mutations occurring in the SARS-CoV-2 RBD, little is known about their impact on receptor recognition, namely hACE2. In this regard, Starr *et al.*[9] have systematically measured the impact of every amino acid in the RBD, by replacing the 20 amino acids in each position, towards hACE2 binding affinity, expressed as the $\Delta\log(K_D)$, in which K_D represents the dissociation constant. Changes in K_D upon single-point mutations were obtained from a deep

[a] *Aggeu Magalhães Institute, Oswaldo Cruz Foundation, Recife, PE, Brazil. E-mail: roberto.lins@cpqam.fiocruz.br*

[b] *Department of Fundamental Chemistry, Federal University of Pernambuco, Recife, PE, Brazil*

† Electronic supplementary information (ESI) available: Associated content includes computational details and sequence data. See DOI: 10.1039/d1cc01747k

‡ These authors contributed equally to this work.

mutational scanning library using the yeast-surface display technique. We have converted the $\Delta\log(K_D)$ into the change in the mutational Gibbs free energy of binding $\Delta\Delta G$ for all sites of interaction between SARS-CoV-2 RBD and hACE2 (more details in ESI†) and observed that whereas most of the single mutations on the RBD tend to be deleterious (*i.e.*, $\Delta\Delta G > 0$), none of the mutations would dramatically enhance the affinity for the hACE2 (Fig. S1, ESI†). Since the wild-type (WT) RBD (from L strain reference genome) binds to the hACE2 in the nanomolar range, variations in the K_D on the order of 1E + 1, resulting in approximately 0.5–1.5 kcal mol^{-1}, do not have the potential to significantly impact the binding affinity. However, it is important to stress that deep mutational scanning binding $\Delta\Delta G$ values were reported for single mutations only and the novel SARS-CoV-2 VOCs often involve more than one mutation on the RBD.

Aiming to investigate whether multiple mutations could lead to a significant increase in affinity to hACE2, variation in binding free energy calculations were performed between the RBDs of selected VOCs and hACE2. For 4 out of 7 lineages evaluated, the binding $\Delta\Delta G$ values fell within the mean absolute error (MAE) associated with the method used, (*ca.*$\pm$1.7 REU, by comparing it to a dataset of more than 4000 mutations from the deep mutational scanning; see the methodology section of the ESI†), whereas the remaining values were positive (*i.e.*, indicating unfavourable binding), but only slightly to the error limit (Fig. 1B). This finding is in agreement with the data derived from the above discussed deep mutational scanning experiments[9] and bio-layer interfeometry assays,[10] where all measurements have shown K_D values for different RBDs to hACE2 within 10^{-8} to 10^{-9} M. Therefore, assumptions that higher transmissibility is mainly associated with mutations in the RBD that leads to an enhanced affinity to hACE2 must be revisited, as both experiments and calculations do not show substantial evidence corroborating this hypothesis.

On the other hand, a plethora of studies has demonstrated antibody evasion for some of the novel VOCs.[11,12] However, data correlating immune evasion of SARS-CoV-2 VOCs with binding free energies are currently not available. In order to evaluate the thermodynamics contribution of such low cross-reactivity, we calculated the variation in binding free energy values for a selected set of SARS-CoV-2 VOC RBDs complexed to 21 known nAbs for which atomic coordinates were made publicly available (Table S2, ESI†). These nAbs bind to two distinct regions of the viral RBD. As shown in Fig. 1A, all nAbs block the RBD access to hACE2; however, classes I and II have a higher spatial overlap with the hACE2 binding site compared to classes III and IV.[13] The variations in binding free energies are shown in Fig. 1B. The data suggest that binding is highly compromised between most nAbs elicited against RBD of previous circulating non-VOC lineages when compared to VOCs RBD, with the only exception being lineage B.1.429. It is important to note that this variant was identified in Portugal and California (USA)[14] at a similar time frame as VOCs B.1.1.7, B.1.351, and P.1, but it has not spread and increased in frequency significantly as the other recognized VOCs did.

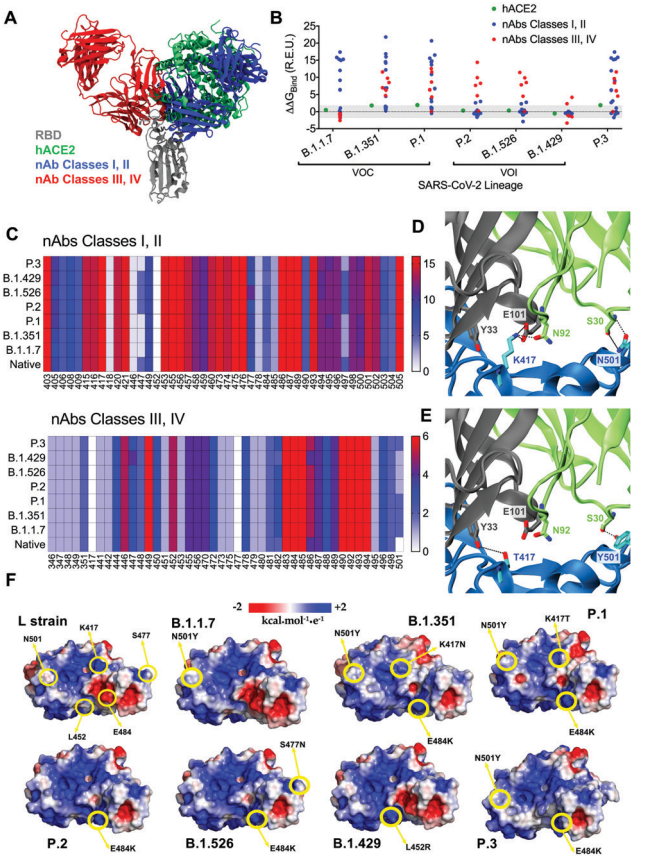

Fig. 1 (A) Cartoon representation of the SARS-CoV-2 RBD (gray) bound to hACE2 (green) and representative nAbs from classes I and II (blue) and III and IV (red); (B) calculated relative binding free energies of RBDs complexed to hACE2 and nAbs (RBD from L strain lineage is taken as reference); (C) map of frequency of contacts of each interface residue of RBD interacting with antibodies from our dataset, shown as a heatmap. Each residue in the RBDs makes at least a single contact (defined as any residue in the RBD interacting within a cutoff distance of 4 Å from the respective nAb). Data for nAb classes I and II are shown on top, whereas classes III and IV are shown on the bottom of the panel. (D) Native ionic and hydrogen bond interactions between the RBD residues K417 and N501 from the L strain lineage (blue) and nAb class I and II (heavy chain shown in gray and light chain shown in green). (E) Loss of interactions between nAbs class I and II upon RBD mutations K417T/N and N501Y, responsible for a large positive $\Delta\Delta G$ variation and loss of cross reactivity with nAbs (protein backbone is represented in cartoon and selected atoms in licorice; carbon atoms are shown in the same colour of their respective chain, oxygen atoms in red and nitrogen atoms in blue; hydrogen atoms were omitted for clarity). (F) Electrostatic surface potential of SARS-CoV-2 RBD reference and selected variants.

Interestingly, the calculated variations in binding free energies are able to capture the trend, *i.e.*, variants that emerged and rapidly reached higher frequencies outcompeting other circulating lineages (VOCs) by having a larger number of nAbs that would not bind to the VOCs. Our calculations also corroborate with available experimental data for nAbs in our dataset. nAbs STE90-C11[15] and C102[13] were verified to continue to bind to RBD containing the E484K mutation (lineage P.2). The calculated $\Delta\Delta G$ for these nAbs against P.2 are within the MAE (Table S2, ESI†). On the other hand, nAb 15033 moderately

loses its neutralization power against a pseudo-virus containing the E484K mutation,[16] a finding supported by a positive $\Delta\Delta G$ variation above the MAE (Table S2, ESI†). As for nAb BD-629, a neutralization assay was performed with the pseudo-virus containing the L452R mutation,[17] which corresponds to lineage B.1.429. It showed that even after the mutation, nAb continues to neutralize the virus, which is also corroborated by our calculations (Table S2, ESI†). It has been also shown that the single mutation N501Y (B.1.1.7) has no impact on the nAb LY-CoV555, while the single mutation E484K (P.2) and the multiple mutations of VOC B.1.351 induce a 1000-fold decrease in neutralization power of the nAb.[18] Our data show that the $\Delta\Delta G$ of LY-CoV555 for B.1.1.7 is within the MAE, while for P.2 and B.1.351, the $\Delta\Delta G$ values are highly positive (Table S2, ESI†), suggesting low affinity and in accordance with the experimental findings. Moreover, our data also suggest that variants B.1.526 and P.2 would have a limited spread as a large number of nAbs are still capable of binding to their RBD and, hence neutralizing it. Conversely, most of the tested nAbs are expected not to bind efficiently to P.3 RBD, a recently reported lineage detected in the Philippines,[19] similar to recognized VOCs B.1.1.7, B.1.351 and P.1, suggesting that this variant is a putative VOC with a high spreading potential in a population with medium to high community immunity against previous circulating lineages due to immune evasion. Another important trend observed in our data is that lineages B.1.1.7, B.1.351 and P.1, which comprise three VOC lineages, have $\Delta\Delta G$ greatly positive against the majority of class I and II nAbs, regardless of the variations for class III and IV nAbs. On the other hand, the $\Delta\Delta G$ values for lineages P.2, B.1.526 and B.1.429 against nAbs classes I and II fall within the SEM of the method. Even though the $\Delta\Delta G$ values for nAbs classes III and IV are highly positive for these latter lineages, they do not become a VOC, being classified only as VOI. This finding suggests that a new lineage is a putative new VOC when its set of mutations leads to immune evasion for most classes I and II nAbs.

To investigate the changes that occur in the interface of interaction between RBD and nAbs, we constructed maps of contact frequency for each RBD interface residue with different classes of nAbs (Fig. 1C). It is worth noting that contacts do not represent the strength of interactions, as unfavourable contacts are also listed. Therefore, we have also been able to identify key antigen–antibody interactions (Fig. S1D and E, ESI†). For class I and II nAbs, native residues K417 and N501 are the ones with the highest frequency of contacts. The K417 residue is important due to the ionic interactions and hydrogen bonds with the nAbs that break when the mutation occurs, while the N501Y change involves the breakdown of the hydrogen bond and the introduction of a bulky residue (Fig. 1D and E). Due to the high frequency of contacts, these changes will impact the binding with most nAbs classes I and II, leading to the immunological evasion of VOCs containing these mutations, including the putative VOC P.3. On the other hand, these residues do not have significant contact frequency with nAbs classes III and IV. Residues S477 and E484 have a moderate frequency of contact with nAbs I and II so that the impact of mutations in these positions on evasion is likely less pronounced. In fact, the E484K mutation alone is not sufficient to classify the P.2 strain as a VOC. In contrast, whereas residue S477 has no impact on the interaction of RBD with nAbs classes III and IV, residue E484 has a high frequency of contact with these nAbs, being involved in ionic interactions that are lost in the mutation and resulting in high $\Delta\Delta G$ values of VOIs P.2 and B.1.426 (see ESI†). Based on our data, the L452 residue is not expected to impact immune evasion due to its low frequency of contact with nAbs class I and II. This observation may explains the fact that lineage B.1.429 has not become a VOC. This residue is important for the recognition of class III and IV nAbs.

Structural analyses revealed that different mechanisms (*e.g.*, loss/change of specific interactions, conformational changes, the introduction of steric clashes) are responsible for lowering the affinity between VOC's RBDs with previously-elicited antibodies. However, it is noteworthy that mutations in VOCs often involve changes in residue charge and/or polarity at the binding interface. As charge distribution on the protein surface is well-known to electrostatically modulate molecular recognition and ligand association,[20,21] the impact of such mutations warrants investigation. Therefore, to further gain insight into the molecular mechanism behind low nAbs cross-reactivity to the VOCs RBD, we have calculated the electrostatic potential of each RBD and plotted it onto their molecular surface (Fig. 1F). The surface charge profile of lineage B.1.429 is remarkably similar to the reference (L strain) lineage, suggesting that the existing nAbs are able to bind to its RBD. In contrast, significant changes in surface charge profile can be seen for the higher spreading variants, especially B.1.351 and P.1. Therefore, in addition to loss/change of specific interactions discussed in the map of contacts, change in global electrostatics will affect overall charge complementary between current nAbs and VOCs RBD.

In this study, levering structural data and computer modelling techniques, we investigated the variation in the binding free-energy ($\Delta\Delta G$) profile of VOC and VOI SARS-CoV-2 lineages with hACE2 and with a dataset of known human nAbs. Our results show only a marginal impact of VOC RBD amino acid changes to hACE2 affinity. This finding, which contrasts to the mechanism that has been proposed earlier,[22] finds support in recent experimental data. On the other hand, we found that VOC RBDs have a significant unfavorable $\Delta\Delta G$ to nAbs classes I and II, and that the energy variation can be related to: (i) changes in residues with a higher frequency of contact with nAbs and involved in important interactions; and (ii) changes in the electrostatic potential surface profiles, hence identifying the molecular and thermodynamical components behind SARS-CoV-2 antibody evasion. In addition, our data suggest that close attention should be given to lineage P.3, as it likely holds high spreading potential in a human population with rising immunity. In summary, the current observed higher transmission of SARS-CoV-2 VOCs is likely to be associated with varying degrees of neutralizing antibody recognition failure in individuals previously exposed to SARS-CoV-2 non-VOC variants. These results have key implications on (i) the basic understanding of VOC emergence and maintenance; (ii) the

rational design of antibody-based therapeutics; (iii) vaccine efficacy and updates; and (iv) may be exploited to rapidly triage newly reported lineages.

R. D. L. and G. W. designed the study. M. V. F. F., E. G. M. and D. F. C. performed all modeling, calculations and data analysis. The manuscript was written with input from all authors.

The authors thank all the health care workers and scientists who have worked hard to deal with this pandemic threat, the GISAID team and all the EpiCoV database's submitters. A GISAID acknowledgment table containing sequences used in this study are attached to this post (Table S3, ESI†). This study was supported by grants from FACEPE, CAPES, CNPq and INCT-FCx and FIOCRUZ COVID-19 Genomic Surveillance Network. Computer allocation was partly granted by the Brazilian National Scientific Computing Center (LNCC). GLW and RDL are supported by the CNPq through their research productivity fellowships (303902/2019-1 and 425997/2018-9).

Conflicts of interest

The authors have declared no competing interests.

Notes and references

1 E. Dong, H. Du and L. Gardner, *Lancet Infect. Dis.*, 2020, **20**, 533–534.
2 P. Zhou, X. L. Yang, X. G. Wang, B. Hu, L. Zhang, W. Zhang, H. R. Si, Y. Zhu, B. Li, C. L. Huang, H. D. Chen, J. Chen, Y. Luo, H. Guo, R. D. Jiang, M. Q. Liu, Y. Chen, X. R. Shen, X. Wang, X. S. Zheng, K. Zhao, Q. J. Chen, F. Deng, L. L. Liu, B. Yan, F. X. Zhan, Y. Y. Wang, G. F. Xiao and Z. L. Shi, *Nature*, 2020, **579**, 270–273.
3 A. Rambaut, N. Loman, O. Pybus, W. Barclay, J. Barrett, A. Carabelli, T. Connor, T. Peacock, D. L. Robertson and E. Volz, *Virological*, 2020, https://virological.org/t/preliminary-genomiccharacterisation-of-an-emergent-sars-cov-2-lineage-in-the-uk-defined-by-a-novel-set-ofspike-mutations/563.
4 H. Tegally, E. Wilkinson, M. Giovanetti, A. Iranzadeh, V. Fonseca, J. Giandhari, D. Doolabh, S. Pillay, E. J. San, N. Msomi, K. Mlisana, A. von Gottberg, S. Walaza, M. Allam, A. Ismail, T. Mohale, A. J. Glass, S. Engelbrecht, G. Van Zyl, W. Preiser, F. Petruccione, A. Sigal, D. Hardie, G. Marais, M. Hsiao, S. Korsman, M. A. Davies, L. Tyers, I. Mudau, D. York, C. Maslo, D. Goedhals, S. Abrahams, O. Laguda-Akingba, A. Alisoltani-Dehkordi, A. Godzik, C. K. Wibmer, B. T. Sewell, J. Lourenco, L. C. J. Alcantara, S. L. Kosakovsky Pond, S. Weaver, D. Martin, R. J. Lessells, J. N. Bhiman, C. Williamson and T. de Oliveira, *Nature*, 2021, **592**, 438–443.
5 N. R. Faria, I. M. Claro, D. Candido, L. A. Moyses Franco, P. S. Andrade, T. M. Coletti, C. A. M. Silva, F. C. Sales, E. R. Manuli and R. S. Aguiar, *Virological*, 2021, https://virological.org/t/genomic-characterisation-of-an-emergent-sars-cov-2-lineage-in-manaus-preliminary-findings/586/2.
6 D. P. Martin, S. Weaver, H. Tegally, E. J. San, S. D. Shank, E. Wilkinson, J. Giandhari, S. Naidoo, Y. Pillay, L. Singh, R. J. Lessells, S. A. Ngs, C.-G. Uk, R. K. Gupta, J. O. Wertheim, A. Nekturenko, B. Murrell, G. W. Harkins, P. Lemey, O. A. MacLean, D. L. Robertson, T. de Oliveira and S. L. K. Pond, 2021, medRxiv:2021.02.23.21252268.
7 N. Felipe, C. Cristiano da, N. Valdinete, S. Victor, C. André, N. Fernanda, C. Ágatha, D. Débora, S. George, M. Matilde, P. Karina, G. Luciana, B. Maria Júlia, J. Michele, S. Marineide, M. Tirza, A. Lígia, S. João Hugo, C.-F. Rubens, S. Tsuyoshi, I. Kentaro, H. Masanori, K. Makoto, S. Marilda Mendonça, W. Gabriel Luz, D. Edson, G. Tiago, B. Gonzalo and R. Paola Cristina, *Research Square*, 2021, DOI: 10.21203/rs.3.rs-318392/v1.
8 A. J. Greaney, A. N. Loes, K. H. D. Crawford, T. N. Starr, K. D. Malone, H. Y. Chu and J. D. Bloom, *Cell Host Microbe*, 2021, **29**, 463–476.
9 T. N. Starr, A. J. Greaney, S. K. Hilton, D. Ellis, K. H. D. Crawford, A. S. Dingens, M. J. Navarro, J. E. Bowen, M. A. Tortorici, A. C. Walls, N. P. King, D. Veesler and J. D. Bloom, *Cell*, 2020, **182**, 1295–1310.
10 X. Zhu, D. Mannar, S. S. Srivastava, A. M. Berezuk, J.-P. Demers, J. W. Saville, K. Leopold, W. Li, D. S. Dimitrov, K. S. Tuttle, S. Zhou, S. Chittori and S. Subramaniam, 2021, bioRxiv:2021.01.11.426269.
11 D. M. Altmann, R. J. Boyton and R. Beale, *Science*, 2021, **371**, 1103–1104.
12 D. Zhou, W. Dejnirattisai, P. Supasa, C. Liu, A. J. Mentzer, H. M. Ginn, Y. Zhao, H. M. E. Duyvesteyn, A. Tuekprakhon, R. Nutalai, B. Wang, G. C. Paesen, C. Lopez-Camacho, J. Slon-Campos, B. Hallis, N. Coombes, K. Bewley, S. Charlton, T. S. Walter, D. Skelly, S. F. Lumley, C. Dold, R. Levin, T. Dong, A. J. Pollard, J. C. Knight, D. Crook, T. Lambe, E. Clutterbuck, S. Bibi, A. Flaxman, M. Bittaye, S. Belij-Rammerstorfer, S. Gilbert, W. James, M. W. Carroll, P. Klenerman, E. Barnes, S. J. Dunachie, E. E. Fry, J. Mongkolsapaya, J. Ren, D. I. Stuart and G. R. Screaton, *Cell*, 2021, **184**, 2348–2361.
13 C. O. Barnes, C. A. Jette, M. E. Abernathy, K. A. Dam, S. R. Esswein, H. B. Gristick, A. G. Malyutin, N. G. Sharaf, K. E. Huey-Tubman, Y. E. Lee, D. F. Robbiani, M. C. Nussenzweig, A. P. West, Jr. and P. J. Bjorkman, *Nature*, 2020, **588**, 682–687.
14 W. Zhang, B. D. Davis, S. S. Chen, J. M. S. Martinez, J. T. Plummer and E. Vail, 2021, medRxiv:2021.01.18.21249786.
15 F. Bertoglio, V. Fühner, M. Ruschig, P. A. Heine, U. Rand, T. Klünemann, D. Meier, N. Langreder, S. Steinke, R. Ballmann, K.-T. Schneider, K. D. R. Roth, P. Kuhn, P. Riese, D. Schäckermann, J. Korn, A. Koch, S. Zock-Emmenthal, M. Becker, M. Scholz, G. M. S. G. Moreira, E. V. Wenzel, G. Russo, H. S. P. Garritsen, S. Casu, A. Gerstner, G. Roth, A. Hermann, T. Schirrmann, S. Dübel, A. Frenzel, J. Van den Heuvel, L. Čičin-Šain, M. Schubert and M. Hust, 2020, bioRxiv:2020.12.03.409318.
16 S. Miersch, Z. Li, R. Saberianfar, M. Ustav, J. B. Case, L. Blazer, C. Chen, W. Ye, A. Pavlenco, M. Gorelik, J. G. Perez, S. Subramania, S. Singh, L. Ploder, S. Ganaie, R. E. Chen, D. W. Leung, P. P. Pandolfi, G. Novelli, G. Matusali, F. Colavita, M. R. Capobianchi, S. Jain, J. B. Gupta, G. K. Amarasinghe, M. S. Diamond, J. Rini and S. S. Sidhu, 2020, bioRxiv:2020.10.31.362848.
17 S. Du, Y. Cao, Q. Zhu, P. Yu, F. Qi, G. Wang, X. Du, L. Bao, W. Deng, H. Zhu, J. Liu, J. Nie, Y. Zheng, H. Liang, R. Liu, S. Gong, H. Xu, A. Yisimayi, Q. Lv, B. Wang, R. He, Y. Han, W. Zhao, Y. Bai, Y. Qu, X. Gao, C. Ji, Q. Wang, N. Gao, W. Huang, Y. Wang, X. S. Xie, X. D. Su, J. Xiao and C. Qin, *Cell*, 2020, **183**, 1013–1023.
18 P. Wang, M. S. Nair, L. Liu, S. Iketani, Y. Luo, Y. Guo, M. Wang, J. Yu, B. Zhang, P. D. Kwong, B. S. Graham, J. R. Mascola, J. Y. Chang, M. T. Yin, M. Sobieszczyk, C. A. Kyratsous, L. Shapiro, Z. Sheng, Y. Huang and D. D. Ho, *Nature*, 2021, **593**, 130–135.
19 F. A. Tablizo, K. M. Kim, C. M. Lapid, M. J. R. Castro, M. S. L. Yangzon, B. A. Maralit, M. E. C. Ayes, E. M. Cutiongco-de la Paz, A. R. D. Guzman, J. M. C. Yap, J.-H. S. Llames, S. M. M. Araiza, K. P. Punayan, I. C. A. Asin, C. F. B. Tambaoan, A. L. U. Chong, K. S. A. R. Padilla, R. P. S. Cruz, E. K. D. Morado, J. G. A. Dizon, R. N. M. Hao, A. A. Zamora, D. R. Pacial, J. A. R. Magalang, M. Alejandria, C. Carlos, A. Ong-Lim, E. M. Salvaña, J. Q. Wong, J. C. Montoya, M. R. Singh-Vergeire and C. P. Saloma, 2021, medRxiv:2021.03.03.21252812.
20 B. Honig and A. Nicholls, *Science*, 1995, **268**, 1144–1149.
21 S. Sivasankar, S. Subramaniam and D. Leckband, *Proc. Natl. Acad. Sci. U. S. A.*, 1998, **95**, 12961–12966.
22 Y. Wang, M. Liu and J. Gao, *Proc. Natl. Acad. Sci. U. S. A.*, 2020, **117**, 13967–13974.